JACS
JOURNAL OF THE AMERICAN CHEMICAL SOCIETY
Communication
pubs.acs.org/JACS

p-Type $CuRhO_2$ as a Self-Healing Photoelectrode for Water Reduction under Visible Light

Jing Gu,[†] Yong Yan,[†] Jason W. Krizan, Quinn D. Gibson, Zachary M. Detweiler, Robert J. Cava, and Andrew B. Bocarsly*

Department of Chemistry, Princeton University, Princeton, New Jersey 08544, United States

Supporting Information

ABSTRACT: Polycrystalline $CuRhO_2$ is investigated as a photocathode for the splitting of water under visible irradiation. The band edge positions of this material straddle the water oxidation and reduction redox potentials. Thus, photogenerated conduction band electrons are sufficiently energetic to reduce water, while the associated valence band holes are energetically able to oxidize water to O_2. Under visible illumination, H_2 production is observed with ~0.2 V underpotential in an air-saturated solution. In contrast, H_2 production in an Ar-saturated solution was found to be unstable. This instability is associated with the reduction of the semiconductor forming Cu(s). However, in the presence of air or O_2, bulk Cu(s) was not detected, implying that $CuRhO_2$ is self-healing when air is present. This property allows for the stable formation of H_2 with ca. 80% Faradaic efficiency.

Direct capture and storage of solar energy via the formation of chemical bonds, by analogy with natural photosynthesis, is a desirable alternate energy approach. One way to reach this goal is to directly convert water to H_2 and O_2, using a photoelectrode that has a photoresponse well matched to the solar spectrum.[1] Hydrogen energy storage is well studied and provides a viable energy resource with minimal environmental impact after combustion.[2] Thus, the capability to design semiconductor photoelectrodes that function as both a photosensitizer and an energy converter, with suitable band edge energies, appropriate spectral response, and good photostability, is of fundamental importance.[3] The majority of photoelectrodes used for water splitting have been *n*-type metal oxides, which act as photoanodes.[4] *p*-Type oxide photocathodes have been the subject of a fewer studies, with noticeable exceptions including $Cu_3Ta_7O_{19}$,[5] $CaFe_2O_4$,[6] Rh modified $SrTiO_3$, and $LuRhO_3$.[7] Still, these materials do not provide the stability combined with good spectral photoresponse and high optical energy conversion efficiency needed for practical water splitting. The development of a high figure of merit, stable, *p*-type photoelectrode would enable a cathodic process for solar energy conversion to hydrogen fuels; a key capability for the development of a self-contained, efficient solar water splitting system.

In addition to the materials noted above, cuprous oxide, which exhibits a *p*-type phase, has been studied as a photocathode. It is an efficient visible light absorber with a conduction band (CB) edge position that meets the thermodynamic requirements for water reduction.[8] However, a major limitation of this material is its redox instability, stemming from its oxidation (Cu_2O/CuO) and reduction (Cu_2O/Cu) potentials, which lie well within the Cu_2O band gap.[9] Cu(I)-based delafossite compounds [Cu(I)-M(III)O_2], which display a relatively small band gap that allows for good overlap with the solar spectrum, provide a more stable alternative to Cu_2O. Structurally, delafossites comprise layers of edge-shared MO_6 octahedra alternating with linear O-Cu(I)-O sticks, similar to what is found in Cu_2O.[10] *p*-Type conductivity in these compounds is readily achieved due to the low formation energy of Cu vacancies (hole producing defects).[11] The increased stability of delafossites as photocathodes is achieved because the electron acceptor orbital is M(III) dominant, with only a small percentage of Cu 3d character. For example, $CuFeO_2$, which contains a Fe(III) dominated CB, was reported to be a photocathode for the reduction of water.[12] Nevertheless, the small percentage of Cu 3d character in the CB of this type of delafossite inevitably results in the formation of a miniscule amount of metallic copper that degrades the efficiency and stability of the system.[13]

We report here the synthesis and photoelectrochemistry of a *p*-type $CuRhO_2$ electrode. Its photostability and water reduction behavior are investigated under air and Ar-saturated solutions in pH = 14 electrolyte. We find that an alkaline electrolyte is preferred, since this environment imbues the electrode with a regenerative capability in the presence of O_2 without having a deleterious impact on H_2 generation. We believe this is the first example of a self-healing semiconductor/electrolyte interface. This introduces a high degree of stability to an electrode that is subject to photoreduction and in so doing produces a system capable of the prolonged photoelectrolysis of water.

The preparation of a polycrystalline $CuRhO_2$ pressed pellet electrode is similar to our previously described method (Supporting Information (SI)).[13] The photocurrent/potential response in a 1 M NaOH electrolyte is shown in Figure 1A. This measurement was carried out under chopped illumination from a 75 W Xe arc lamp (USHIO UXL151H, 350−760 nm using UV and NIR cutoff filters, 49.5 mW/cm^2). Photocurrent starts to flow at ~ −0.1 V vs SCE. We take this potential as an approximation of the electrode's flat band potential in the described electrolyte. Figure 1A illustrates the photocurrent obtained from a freshly prepared electrode under both air- and Ar-saturated electrolyte conditions. No obvious photocurrent difference was observed between these gas saturated electrolytes

Received: September 4, 2013
Published: December 30, 2013

   dx.doi.org/10.1021/ja408876k | *J. Am. Chem. Soc.* 2014, 136, 830−833

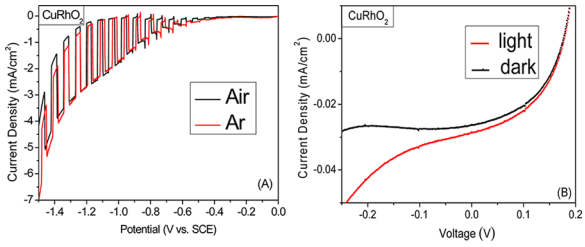

Figure 1. (A, left) Linear sweep voltammetry with a freshly made $CuRhO_2$ electrode measured under chopped light in 1 M NaOH purged with Ar (red) and air (black) (scan rate, 100 mV/s). (B, right) Linear sweep voltammograms at 20 mV/s for a two-electrode cell with no resistance compensation.

(a similar observation was made using a pure oxygen atmosphere, SI Figure S1).

The photoaction spectrum of the cell (Figure 2A) was obtained by determining the incident photon-to-current

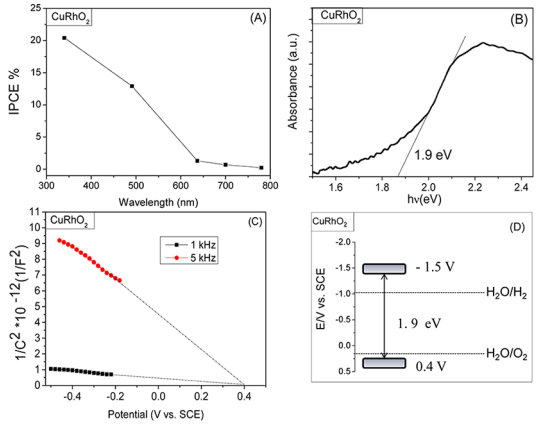

Figure 2. (A) IPCE plots obtained at −0.9 V vs SCE under the air-saturated condition. (B) UV/vis/NIR absorption spectrum of $CuRhO_2$. (C) Mott−Schottky plots at 1 kHz and 5 kHz measured under dark conditions. (D) The CB and VB positions of $CuRhO_2$ compared with the water redox potentials at pH = 14.

conversion efficiency (IPCE) at −0.9 V. The photon current response initiates at ca. 650 nm, consistent with the band gap (~1.9 eV) inferred from the absorption spectrum (see above), with an IPCE of 1%, and reaches ca. 20% at 350 nm. This wavelength range represents ~57% of the AM 1.5 insolation. Thus, the IPCE plot suggests that solar illumination can induce sufficient electron−hole generation and charge separation at the semiconductor/electrolyte interface to drive water reduction. Diffuse reflectance measurements were performed on $CuRhO_2$ powder, as shown in Figure 2B. The band gap was found by extrapolation of the absorption edge; it is estimated to be 1.9 eV. A dependable value of the flat band potential was determined from the dependence of the electrode open-circuit voltage (E_{oc}) on the illumination intensity. E_{oc} reaches a limiting plateau at the flat band potential, yielding ca. +0.4 V (SI Figure S2). Mott−Schottky plots are shown in Figure 2C. The negative slopes of the plots further confirmed *p*-type behavior of the electrode. The flat band potential, V_{fb}, as determined from the frequency independent *x*-axis intercept of the Mott−Schottky plots, is +0.43 V. This value is close to the value obtained using the open-circuit photovoltage measurements but is not consistent with the estimated flatband potential (−0.1 V) based on the current onset in the current/potential curve (Figure 1A). This discrepancy indicates a kinetic bottleneck in the charge transfer process. Efficient electron−hole separation should only require ~300 mV of band bending. However, in the present case, the potential difference between band bending onset (i.e., the flatband potential) and the observation of photocurrent is 500 mV. This displacement suggests a high overpotential for the electron transfer from the conduction band to the redox active species (H_2O). Note also that there is a relatively large frequency dispersion in the Mott−Shottky data, suggesting that a surface state population impacts the interfacial charge transfer process.[14] Given the fact that the material employed is highly doped (3×10^{19} cm^{-3}, SI),[14] the valence band (VB) edge energy (E_{vb}) is reasonably estimated to be within 100 mV of the flatband potential (0.4 V). The 1.9 eV band gap then places the CB edge energy (E_{cb}) at −1.5 V, as illustrated in Figure 2D. Thus, the CB of this semiconductor sits at a potential that meets the thermodynamic requirement for the reduction of water (−1.08 V) while the $CuRhO_2$ VB edge lies at a potential sufficiently positive to oxidize water (0.15 V), as summarized in Figure 2D. Given these energetics, the $CuRhO_2$ photoelectrode is a good candidate for visible light induced water splitting. This conclusion is experimentally confirmed by the current vs cell bias plot shown in Figure 1B. This data was collected using a two electrode configuration in which a regulated voltage power supply was superimposed between the $CuRhO_2$ photocathode and a platinum mesh anode. The system was not optimized for resistive losses. Note that, though small, there is a distinct photocurrent at zero bias, which is associated with the observation of the formation of bubbles on both electrodes. Thus, this system splits water under visible irradiation without an externally applied voltage. Thermodynamically, the decomposition of water to H_2 and O_2 requires 1.23 V of bias across the electrodes. However, in the present system a bias of only 200 mV generates a photocurrent ~0.025 mA/cm^2. Thus, solar fuel formation is obtainable using a *p*-$CuRhO_2$ photocathode and a dark anode. A minor dark current is observed at zero bias in either air (Figure 1B) or Ar condition, which may result from slow electrode decomposition. Analysis of the time dependence of the dark current at zero bias suggests a Faradaic process.

To investigate the photophysics of excited state electron transfer between the VB and CB in this material, electronic-structure calculations were performed on the experimentally determined structure[15] using density functional theory. The corresponding total and partial densities of states, band gap, and band structure are shown in SI Figure S3. The CB of $CuRhO_2$ is dominated by Rh 4d states that are mixed slightly with O 2p states, while the higher energy region of the VB is mainly composed of the Cu 3d state blending with Rh 4d and O 2p states. An indirect band gap energy of ca. 1.5 eV is found, which is in reasonable agreement with the experimental value of 1.9 eV. Globally, the DFT calculations characterize the lowest energy band to band transition in $CuRhO_2$ as a metal to metal charge transfer transition from Cu 3d to Rh 4d, which is anticipated to stabilize the illuminated semiconductor by protecting the metal−oxygen bonds.[16] The system is further protected by the instability of the photoexcited Rh(II) oxidation state compared to the highly stable Rh(III) ground state.

Experiments testing the photoelectrochemical reduction of water using the $CuRhO_2$ electrode under visible light irradiation were conducted holding the electrode potential at −0.9 V vs SCE in 1 M NaOH, exposed to air, for more than 8 h. This potential is ca. 0.2 V less than the thermodynamic potential of water reduction (−1.08 V). The production of H_2 gas was visualized

dx.doi.org/10.1021/ja408876k | J. Am. Chem. Soc. 2014, 136, 830−833

through the formation of bubbles at the surface of the electrode and confirmed by gas chromatography. These experiments were carried out in solutions exposed to air, but the system was not sparged during the electrolysis. Air presaturation of the electrolyte was sufficient to maintain a constant current for at least 8 h. The amount of H_2 evolution under air and Ar-saturated conditions is compared in Figure 3C. H_2 production under air

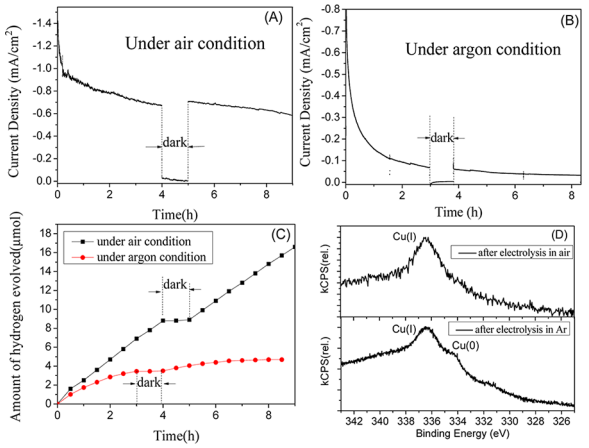

Figure 3. (A) Photoelectrolysis: cathodic current density vs time in an air-saturated solution. (B) Photoelectrolysis: cathodic photocurrent density vs time in an Ar-saturated solution. (C) H_2 evolution using $CuRhO_2$ as a photocathode with an applied potential of −0.90 V in Ar- or air-saturated 1 M NaOH solutions under visible light irradiation. (D) XPS characterization of $CuRhO_2$ electrodes surface after electrolysis under air and Ar.

continuously increases up to ca. 17 μmol during the electrolysis, unless the illuminating light was blocked, which immediately stopped the gas production (Figure 3AC), thus directly correlating H_2 evolution with the photoresponse of the semiconductor electrode.

An ∼80% Faradaic efficiency was calculated based on the collection of H_2 gas under the air-saturated conditions (SI). This value was invariant over an 8 h reaction period (Figure 3C); the longest time period tested. In contrast, the rate of H_2 production in the Ar-saturated case dramatically decreases during the first 1−2 h, and the catalytic activity almost disappears after ∼3 h of electrolysis (Figure 3BC). The continuously decreasing current shown in Figure 3B is characteristic of electrode surface deactivation via a decomposition pathway. In the present case, this process reduces the current under Ar to 10% of the current observed under air after a 3-h electrolysis. To obtain a stable H_2 generating system, we find that two criteria must be met: the electrolyte must be saturated with O_2 (either from air or a pure oxygen stream, and the pH of the electrolyte must be basic). The improved stability of the electrode in air suggests the presence of an interfacial self-regeneration mechanism.

To investigate this effect, materials analyses of pre- and postelectrolysis electrodes were undertaken. Powder X-ray diffraction (XRD) characterization (SI Figure S4) showed no apparent crystal structure change (all peaks belong only to $CuRhO_2$), indicating that the bulk phase of the electrodes did not change independent of whether the electrolysis was conducted under Ar or under air. However, SEM analysis indicates a change in surface morphology from well-defined crystallites prior to electrolysis to larger particles when an Ar atmosphere is employed. Little change is observed during electrolysis under air (SI Figure S5). EDX analysis of pre- and postelectrolysis electrodes, where the experiment was carried out under Ar, yielded a dramatic change in the Cu/Rh ratio (SI Figure S6). The EDX results obtained from electrodes utilized under Ar indicated a near surface Cu to Rh ratio of 1.7:1, while electrodes run in an air saturated electrolyte yielded a 1.1:1 ratio. The higher ratio of Cu to Rh after electrolysis suggests the surface accumulation of metallic Cu reduced from Cu(I) under the electrolysis conditions. This finding was confirmed by XPS, which yielded a Cu(0) Auger peak for electrodes run under Ar that was absent in both pre-electrolysis electrodes and electrodes run under air (SI Figure S7 and Figure 3D).

To confirm that the stability of the electrode is induced by oxygen, chopped light electrolysis currents were plotted against electrolysis time under air, Ar, and mixed gas (air/Ar = 1:1) as shown in SI Figure S8. During the 30 min electrolysis time employed, ∼98% of the photocurrent is maintained in the air-saturated solution. In comparison, the photocurrent decreases by 55% under Ar-saturated conditions. Approximately 15% of the photocurrent is lost under the mixed gas conditions. These results indicate that ∼0.3 mmol/L of dissolved O_2 in the solution is enough to stabilize the electrode surface; decreased concentration of O_2 results in electrode destabilization, but increased concentration up to the pure oxygen saturated (1.4 mmol/L) condition shows no obvious improvement (SI Figure S1).

Chopped light, linear sweep voltammograms were recorded after different electrolysis times under air and Ar atmospheres (0 h, 1 h, 8 h), showing the differential stability of the air-based systems over the Ar-based systems. Prior to electrolysis, the photocurrent densities of two electrodes were similar (Figure 4A). However, after 1 h (Figure 4B), a clear decrease in

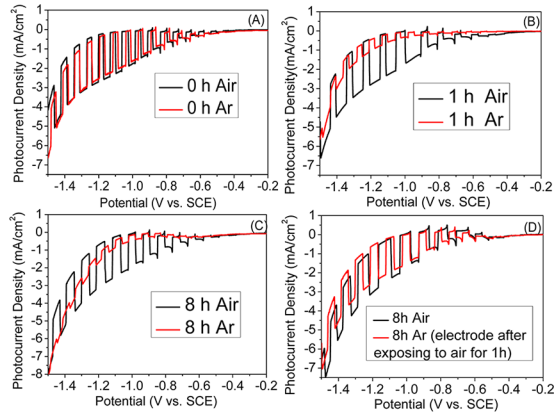

Figure 4. Linear sweep voltammetry of $CuRhO_2$ electrodes: (A) before electrolysis under chopped light conditions; (B) after electrolysis for 1 h; (C) after electrolysis for 8 h. (D) The electrode, after electrolysis for 8 h was exposed to air for 1 h at 100 °C.

photocurrent was observed in the Ar case (∼70% current loss) while no apparent change in photocurrent was observed for the air case. This difference was manifest at t = 8 h also (Figure 4C). When the deactivated electrode obtained after 8 h electrolysis in Ar was heated in air for 1 h (100 °C), as shown in Figure 4D, ∼95% of the photocurrent was recovered. Reactivation was only achieved when oxygen was present. It is concluded that exposure to O_2 via a postreaction thermal treatment reforms the $CuRhO_2$ interface. When O_2 is present in the electrochemical cell, it either inhibits the formation of Cu(s) or rapidly reacts with trace

dx.doi.org/10.1021/ja408876k | J. Am. Chem. Soc. 2014, 136, 830−833

quanitites of copper metal to regenerate $CuRhO_2$. Alternatively, photoproduced copper metal might react with O_2 to form a surface layer of Cu_2O. However, we rule this out in the present case, since p-Cu_2O electrodes have been reported to be unstable on a 20 min time scale.[9] This is inconsistent with the behavior reported in Figures 3 and 4. Finally, we note that control experiments using a p-Cu_2O photocathode generate a surface layer of copper metal even when run under air that is photoelectrochemically deleterious (SI Figure S8). Thus, the transformation of a p-$CuRhO_2$ surface to a p-CuO_2 surface is inconsistent with the data available, while preservation of the $CuRhO_2$ interface via reaction with O_2 is well supported.

p-$CuFeO_2$ is the only previously studied delafossite electrode reported to carry out a reductive process in the presence of aqueous oxygen.[12] In this case, oxygen was proposed to function as the major electron acceptor excluding H_2 as a reduction product.[12,17] The $CuRhO_2$ system is fundamentally different, with water reduction preferred over oxygen reduction. Since both of these processes are thermodynamically allowed under the conditions employed, there must be a kinetic advantage for H_2 production at the $CuRhO_2$ interface. Electrode stabilization is then associated with a totally separate chemical redox process. Four reactions that can hypothetically occur at the cathode are proposed. The first three processes are purely electrochemical. We have already argued that reaction 1 is more facile in this system than reaction 2, since, experimentally we see that 80% of the electrons are channeled through reaction 1. Reaction 3 represents the electrode decomposition pathway under Ar. The final reaction provides the self-healing property. It is a pure redox reaction between dissolved O_2 and the surface Cu atoms. This reaction requires a basic electrolyte to move O_2 redox potential to a value where the surface Cu species can be oxidized. Note that this reaction could not occur if reaction 2 proceeded at a significant rate.

$$2H_2O + 2e^- \rightarrow H_2 + 2OH^- \quad (1)$$

$$O_2 + 2H_2O + 4e^- \rightarrow 4OH^- \quad (2)$$

$$Cu(I)^* + e^- \rightarrow Cu_{surf}(0) \quad (3)$$

$$Cu_{surf}(0) + {}^1/_4O_2 + {}^1/_2H_2O \rightarrow Cu(I)^* + OH^- \quad (4)$$

In conclusion, we have shown that a $CuRhO_2$ delafossite photocathode, with a strong visible light response and innately p-type semiconductor character, is an excellent candidate for water reduction. Polycrystalline electrodes can be prepared by straightforward solid-state methods, and water reduction with this electrode under visible-light irradiation is achieved at an underpotential of ~0.2 V in 1 M NaOH. A photocurrent up to -1.0 mA/cm^2 at -0.9 V was achieved in air with the electrode exhibiting stability for at least 8 h. We believe this to be the first example of an oxygen driven self-healing process at an electrode/electrolyte interface. Of equal importance is the finding that the p-$CuRhO_2$ electrode has band edges that straddle the water oxidation and reduction processes, while responding to visible light. Thus, this material is a prime candidate for generating solar fuels from water.

■ ASSOCIATED CONTENT

Ⓢ Supporting Information

Experimental details and characterization data. This material is available free of charge via the Internet at http://pubs.acs.org.

■ AUTHOR INFORMATION

Corresponding Author

bocarsly@princeton.edu

Author Contributions

[†]J.G. and Y.Y. contributed equally.

Notes

The authors declare no competing financial interests.

■ ACKNOWLEDGMENTS

The authors acknowledge support of this research from the Office of Basic Energy Sciences, Department of Energy. The solid-state synthesis and physical characterization of materials were carried out under the direction of R.J.C. under Grant DE-FG02-98ER45706. Photoelectrochemical experiments and analysis were carried out under the direction of A.B.B. under Grant DE-SC0002133.

■ REFERENCES

(1) Halacy, D. S. *The coming age of solar energy*; Harper & Row: New York, 1973.

(2) Dunn, S. *Int. J. Hydrogen Energy* **2002**, *27*, 235.

(3) (a) Walter, M. G.; Warren, E. L.; McKone, J. R.; Boettcher, S. W.; Mi, Q.; Santori, E. A.; Lewis, N. S. *Chem. Rev.* **2010**, *110*, 6446. (b) Mayer, M. T.; Lin, Y.; Yuan, G.; Wang, D. *Acc. Chem. Res.* **2013**, *46*, 1558. (c) Maeda, K.; Teramura, K.; Lu, D.; Takata, T.; Saito, N.; Inoue, Y.; Domen, K. *Nature* **2006**, *440*, 295. (d) Maeda, K.; Domen, K. *J. Phys. Chem. C* **2007**, *111*, 7851.

(4) (a) Tachibana, Y.; Vayssieres, L.; Durrant, J. R. *Nat. Photonics* **2012**, *6*, 511. (b) Sun, J.; Zhong, D. K.; Gamelin, D. R. *Energy Environ. Sci.* **2010**, *3*, 1252. (c) Mohamed, A. E. R.; Rohani, S. *Energy Environ. Sci.* **2011**, *4*, 1065. (d) Linsebigler, A. L.; Lu, G.; Yates, J. T., Jr. *Chem. Rev.* **1995**, *95*, 735.

(5) (a) Fuoco, L.; Joshi, U. A.; Maggard, P. A. *J. Phys. Chem. C* **2012**, *116*, 10490. (b) Joshi, U. A.; Palasyuk, A.; Arney, D.; Maggard, P. A. *J. Phys. Chem. Lett.* **2010**, *1*, 2719. (c) Woodhouse, M.; Parkinson, B. A. *Chem. Mater.* **2008**, *20*, 2495.

(6) Ida, S.; Yamada, K.; Matsunaga, T.; Hagiwara, H.; Matsumoto, Y.; Ishihara, T. *J. Am. Chem. Soc.* **2010**, *132*, 17343.

(7) (a) Iwashina, K.; Kudo, A. *J. Am. Chem. Soc.* **2011**, *133*, 13272. (b) Jarrett, H. S.; Sleight, A. W.; Kung, H.; Gillson, J. L. *J. Appl. Phys.* **1980**, *51*, 3916. (c) Jarrett, H. S.; Sleight, A. W.; Kung, H.; Gillson, J. L. *Surf. Sci.* **1980**, *101*, 205.

(8) (a) Sowers, K. L.; Fillinger, A. *J. Electrochem. Soc.* **2009**, *156*, F80. (b) Engel, C. J.; Polson, T. A.; Spado, J. R.; Bell, J. M.; Fillinger, A. *J. Electrochem. Soc.* **2008**, *155*, F37.

(9) Paracchino, A.; Laporte, V.; Sivula, K.; Grätzel, M.; Thimsen, E. *Nat. Mater.* **2011**, *10*, 456.

(10) (a) Marquardt, M. A.; Ashmore, N. A.; Cann, D. P. *Thin Solid Films* **2006**, *496*, 146. (b) Shannon, R. D.; Rogers, D. B.; Prewitt, C. T.; Gillson, J. L. *Inorg. Chem.* **1971**, *10*, 723.

(11) (a) Nagarajan, R.; Duan, N.; Jayaraj, M.; Li, J.; Vanaja, K.; Yokochi, A.; Draeseke, A.; Tate, J.; Sleight, A. *Int. J. Inorg. Mater.* **2001**, *3*, 265. (b) Raebiger, H.; Lany, S.; Zunger, A. *Phys. Rev. B* **2007**, *76*, 045209.

(12) Read, C. G.; Park, Y.; Choi, K.-S. *J. Phys. Chem. Lett.* **2012**, *3*, 1872.

(13) (a) Gu, J.; Wuttig, A.; Krizan, J. W.; Hu, Y.; Detweiler, Z. M.; Cava, R. J.; Bocarsly, A. B. *J. Phys. Chem. C* **2013**, *117*, 12415. (b) Yan, Y.; Zeitler, E. L.; Hu, Y.; Bocarsly, A. B. *J. Am. Chem. Soc.* **2013**, *135*, 14020.

(14) Finklea, H. O. *Semiconductor electrodes*; Elsevier: 1988.

(15) Capobianco, C. J.; Drake, M. J. *Geochim. Cosmochim. Acta* **1990**, *54*, 869.

(16) Thurston, T.; Wilcoxon, J. *J. Phys. Chem. B* **1999**, *103*, 11.

(17) de Jongh, P.; Kelly, J. *Chem. Commun.* **1999**, 1069.

■ NOTE ADDED AFTER ASAP PUBLICATION

Figure S8 was added to the Supporting Information, and the new version was posted on January 13.